

## Organocatalysis

International Edition: DOI: 10.1002/anie.201901346  
German Edition: DOI: 10.1002/ange.201901346

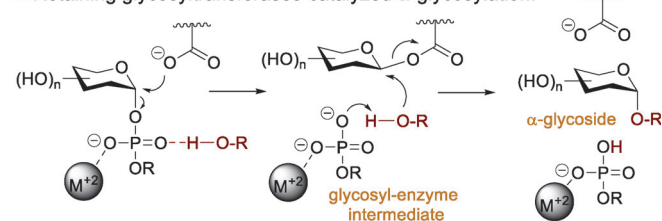
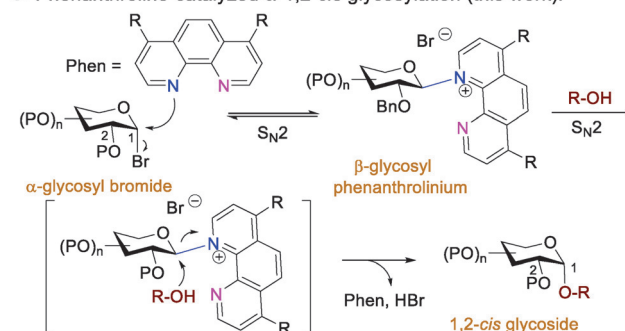
## Phenanthroline-Catalyzed Stereoretentive Glycosylations

Fei Yu, Jiayi Li, Paul M. DeMent, Yi-Jung Tu, H. Bernhard Schlegel, and Hien M. Nguyen\*

**Abstract:** Carbohydrates are essential moieties of many bioactive molecules in nature. However, efforts to elucidate their modes of action are often impeded by limitations in synthetic access to well-defined oligosaccharides. Most of the current methods rely on the design of specialized coupling partners to control selectivity during the formation of glycosidic bonds. Reported herein is the use of a commercially available phenanthroline to catalyze stereoretentive glycosylation with glycosyl bromides. The method provides efficient access to  $\alpha$ -1,2-*cis* glycosides. This protocol has been performed for the large-scale synthesis of an octasaccharide adjuvant. Density-functional theory calculations, together with kinetic studies, suggest that the reaction proceeds by a double  $S_N2$  mechanism.

Glycosylations are fundamental methods for constructing complex carbohydrates. Key reactions involve glycosidic bond formation that connects glycosyl electrophiles to glycosyl nucleophiles to generate oligosaccharides, which play a critical role in cellular functions and disease processes.<sup>[1]</sup> As a result, the efficient preparation of well-defined oligosaccharides has been a major focus in carbohydrate synthesis. Despite recent advances,<sup>[2]</sup> the ability to forge  $\alpha$ -1,2-*cis* glycosidic bonds in a stereoselective fashion is not easily predictable (Scheme 1A) because of the reaction's high degree of variables and shifting  $S_N1$ - $S_N2$  mechanistic paradigm.<sup>[3]</sup> Most established methods have focused on tuning the steric and electronic nature of the protecting groups bound to the electrophilic partners to achieve  $\alpha$ -1,2-*cis* selectivity.<sup>[4]</sup> Recently, catalyst-controlled methods have emerged as a way to eliminate the need for the design of specific glycosyl electrophiles.<sup>[5]</sup> Although catalytic glycosylations concentrate on the use of catalysts to control the desired stereochemistry, only limited examples for forming  $\alpha$ -1,2-*cis* glycosides are known.<sup>[5d]</sup>

To identify an effective strategy for a stereoselective synthesis of  $\alpha$ -1,2-*cis* glycosides that would obviate the necessity for substrate prefunctionalization, we considered whether the anomeric selectivity could be controlled by a simple catalyst. We recognized that retaining glycosyltransferases are known to catalyze  $\alpha$ -glycosidic bond formation with the net retention of the anomeric configuration (Scheme 1B).<sup>[6]</sup> As such, we envisioned that a catalyst capable of

A. General structures of 1,2-*cis*- and 1,2-*trans*-glycosidic bonds:B. Retaining glycosyltransferases-catalyzed  $\alpha$ -glycosylation:C. Phenanthroline-catalyzed  $\alpha$ -1,2-*cis* glycosylation (this work):

Scheme 1. Introduction and synopsis of current work.

acting as a glycosyltransferase to provide 1,2-*cis* glycosides, with predictable  $\alpha$ -selectivity and high yields, would likely find broad applications. Pyridine has been reported by Lemieux and Morgan to serve as a nucleophilic catalyst to displace the anomeric leaving group of a glycosyl electrophile.<sup>[7]</sup> The glycosyl pyridinium ion formed in the reaction prefers the equatorial position to avoid the steric and electrostatic interactions associated with positioning that group in the axial orientation.<sup>[7]</sup> Inversion by nucleophilic substitution would then afford an  $\alpha$ -1,2-*cis* glycoside. However, it was apparent from the outset of our studies that the adaptation of the pyridine system could present challenges. As an axial pyridinium ion can also be generated, from the reaction of an electrophile with pyridine, to compete for access to  $\beta$ -1,2-*trans* glycoside,<sup>[7,8]</sup> a pyridine-mediated reaction proceeds with marginal bias for the  $\alpha$ -selectivity. Herein, we report the discovery of a commercially available phenanthroline to stereoselectively catalyze formation of  $\alpha$ -1,2-*cis* glycosides (Scheme 1C). Phenanthroline is a rigid and planar structure with two fused pyridine rings whose nitrogen atoms are positioned to act cooperatively. We postulated that the first nitrogen atom serves as a catalytic nucleophile to react with an electrophile to generate a covalent  $\beta$ -glycosyl phenanthrolium ion preferentially, as phenanthroline is more sterically demanding than pyridine. The second nitro-

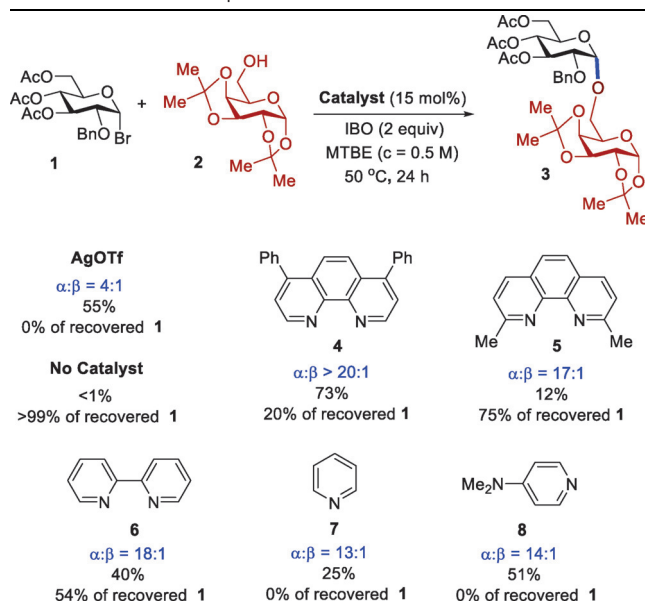
\*] Dr. F. Yu, J. Li, P. M. DeMent, Dr. Y.-J. Tu, Prof. H. B. Schlegel, Prof. H. M. Nguyen  
Department of Chemistry, Wayne State University  
Detroit, MI 48202 (USA)  
E-mail: hmnguyen@wayne.edu

Supporting information and the ORCID identification number(s) for the author(s) of this article can be found under:  
<https://doi.org/10.1002/anie.201901346>.

gen atom could either noncovalently interact with the carbohydrate moiety or form a hydrogen bond with the alcohol nucleophile to facilitate substitution. These features should effectively promote a double  $S_N2$  mechanism.

To initiate our investigation, the  $\alpha$ -glycosyl bromide **1** was chosen as a model electrophilic partner and the galactopyranoside **2** as a nucleophile to simplify the analysis of coupling product mixtures (Table 1). Previous reports have docu-

**Table 1:** Reaction development.<sup>[a]</sup>



[a] The reaction was conducted with 0.2 mmol of **1** and 0.4 mmol of **2**. Yields of isolated products averaged three runs. The ( $\alpha/\beta$ ) ratios were determined by  $^1\text{H}$  NMR analysis.

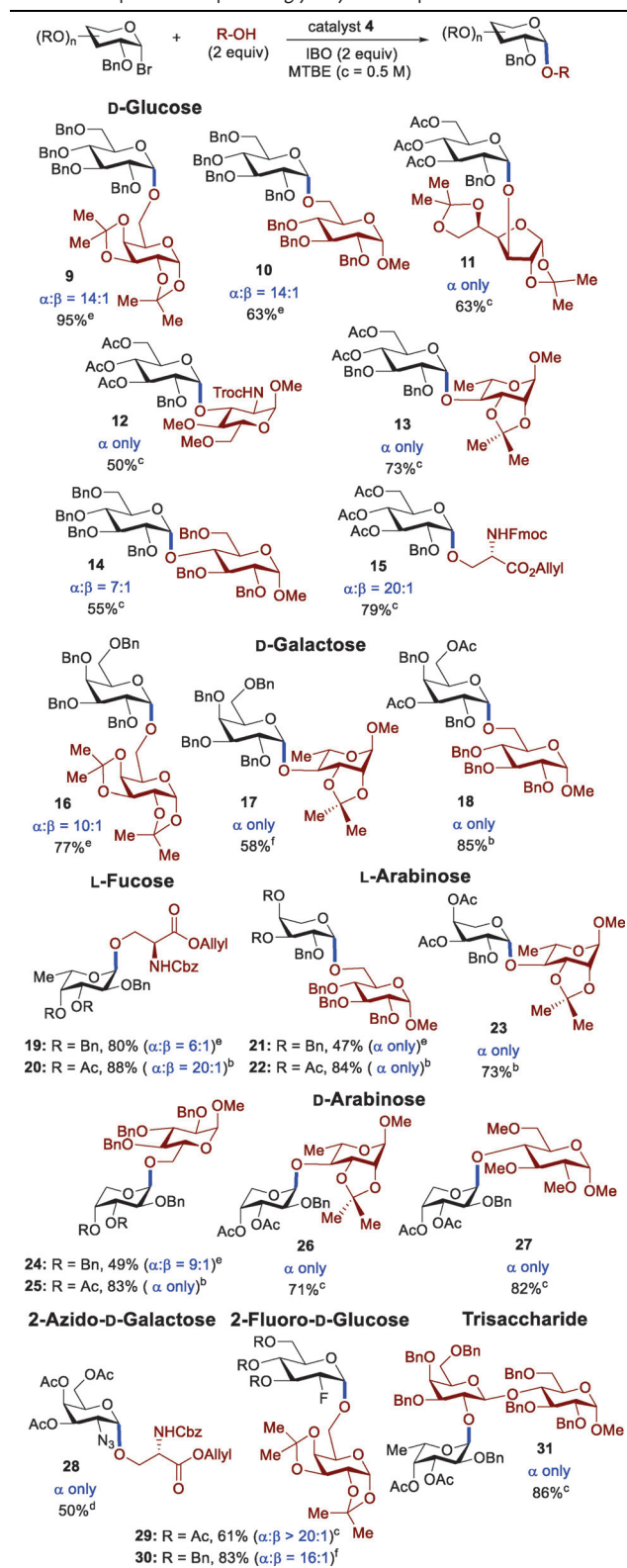
mented the ability of glycosyl bromides to function as effective electrophiles under various reaction conditions.<sup>[9]</sup> The reaction of **2** with **1**, having a C2 benzyl (Bn) group,<sup>[2]</sup> often proceeds by an  $S_N1$ -like pathway. As expected, use of a Lewis acid, silver triflate (AgOTf), provided a 4:1 ( $\alpha/\beta$ ) mixture of the disaccharide **3**. Upon exploring a wide range of reaction parameters (see Figures S1–S6 in the Supporting Information), we discovered that coupling of **2** with **1** with 15 mol % of 4,7-diphenyl-1,10-phennathroline (**4**) as a catalyst and isobutylene oxide (IBO) as a hydrogen bromide scavenger in *tert*-butyl methyl ether (MTBE) at 50 °C for 24 hours provides the highest yield and selectivity of **3** (73%,  $\alpha/\beta > 20:1$ ). In the absence of **4**, no reaction was apparent after 24 hours. We also conducted the reaction with the catalysts **5**–**8**, and three trends are observed. First, the yield of **3** is correlated with the ability of the catalyst to displace the C1 bromide. The C2 and C9 methyl groups of **5** reduce the accessibility of the pyridine nitrogen atom for displacing the anomeric bromide. Second, the catalyst's conformation can influence the efficiency and selectivity. For instance, 2,2'-bipyridine (**6**) is less  $\alpha$ -selective than **4** potentially because of the position of the two nitrogen atoms resulting from the free rotation about the bond linking the pyridine rings. Third, the selectivity is correlated with the efficiency of the catalyst. As

expected, pyridine (**7**) is not as selective as **4**. Since 4-(dimethylamino)pyridine (**8**) is a more effective catalyst than **7**,<sup>[10]</sup> **3** was obtained in higher yield. To explore if this catalytic system could be suitable for a large-scale synthesis, we examined the reaction on a 4 mmol scale of **1** and 4.4 mmol of **2**. At high concentration (2 M), use of 5 mol % **4** proved sufficient to provide **3** (70%,  $\alpha/\beta > 20:1$ ; see Figure S7).

There are several underlying factors that potentially influence the efficiency and the selectivity of the coupling products, including the protecting groups of glycosyl electrophiles,<sup>[2–4]</sup> the reactivity of the nucleophiles, and the reaction conditions. As a result,  $\alpha$ -1-bromo electrophiles were investigated (Table 2). To validate that **4** could overturn the “remote” participation of the C3, C4, and C6 acyl protecting groups, we first explored the coupling with glucosyl bromides having non-participatory benzyl protecting groups. No significant compromise to the  $\alpha$ -selectivity was observed for the disaccharides **9** and **10** with use of tetrabenzyl glucosyl bromide. This protocol is more  $\alpha$ -selective than other approaches. For example, while our system provided **10** with  $\alpha/\beta = 14:1$ , TMSOTf-mediated coupling with imidate electrophiles provided **10** with marginal  $\alpha$  selectivity ( $\alpha/\beta = 1:1.2–4:1$ ).<sup>[11]</sup> In addition, these glucosyl bromides effectively coupled secondary alcohols to afford **11–13** with high  $\alpha$ -selectivity. For the challenging C4 hydroxy, the  $S_N1$ – $S_N2$  reaction paradigm was slightly shifted (**14**:  $\alpha/\beta = 7:1$ ). A protected serine nucleophile also exhibited high  $\alpha$ -selectivity (**15**:  $\alpha/\beta = 20:1$ ).

Next, we investigated the ability of **4** to overturn the inherent bias of D-galactose, whose axial C4 benzyl group has been reported to favor  $\beta$ -product formation.<sup>[12]</sup> Under our catalytic system, galactosyl bromides served as effective electrophiles to deliver **16–18** (Table 2) with high  $\alpha$ -selectivities. In contrast, the amide-promoted reaction provided **16** with  $\alpha/\beta = 3:1$ .<sup>[13]</sup> We discovered that while tribenzyl L-fucosyl bromide afforded **19** with  $\alpha/\beta = 6:1$ , use of triacetyl L-fucose provided exclusively  $\alpha$ -**20**. Both **19** and **20** are key units of a thrombospondin type 1 compound associated with an autosomal recessive disorder.<sup>[14]</sup> Use of tribenzyl L-arabinosyl bromide also provided exclusively  $\alpha$ -**21**, albeit with 47 % yield because of decomposition during the course of the reaction. The yield could be improved with use of the acetyl protecting groups (**22**: 84 %). The diacetyl L-arabinose was compatible with a C4 hydroxy group to afford  $\alpha$ -**23**.<sup>[15]</sup> A similar trend was observed with D-arabinose (**24–27**). For comparison, this protocol to produce **24** ( $\alpha/\beta = 9:1$ ) is more  $\alpha$ -selective than the thioglycoside method employing NIS/AgOTf as the activating agent ( $\alpha/\beta = 3:1$ ).<sup>[15]</sup>

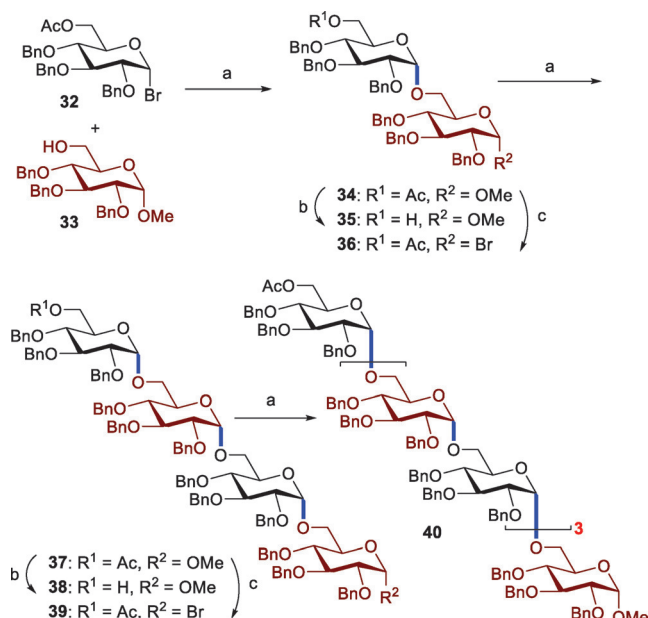
We also sought to explore the selectivity trends with electrophiles bearing C2 azido and C2 fluoro groups (Table 2). Use of the C2 azido galactose substrate provided exclusively  $\alpha$ -**28**, a tumor-associated mucin  $T_N$  antigen precursor.<sup>[16]</sup> To compare, **28** had been previously prepared as a 4:1 ( $\alpha/\beta$ ) mixture using AgClO<sub>4</sub> as the activating reagent.<sup>[17]</sup> Next, we turned our attention to a 2-fluoro-D-glucose substrate. The ability of the C2–F bond to have an impact on the stereochemistry of the product has been reported.<sup>[18]</sup> While the 2-fluoro-glucose having benzyl protecting groups is highly  $\beta$ -selective under TMSOTf-mediated

**Table 2:** Scope with respect to glycosyl electrophiles.<sup>[a]</sup>

[a] All reactions were conducted on a 0.15–0.3 mmol of glycosyl bromides. Yields of isolated products averaged over two to three runs. The ( $\alpha/\beta$ ) ratios were determined by <sup>1</sup>H NMR analysis. [b] 15 mol% **4**, 24 h, 50 °C. [c] 30 mol% **4**, 24–48 h, 50 °C. [d] 50 mol% **4**, 50 °C, 48 h. [e] 20 mol% **4**, 25 °C, 24–48 h. [f] 20 mol% **4**, 50 °C, 24 h.

reactions, the analogous acetyl electrophile affords a 1:1 ( $\alpha/\beta$ ) mixture. In contrast, both substrates are  $\alpha$ -selective under phenanthroline conditions (**29**,  $\alpha/\beta > 20:1$ ; **30**,  $\alpha/\beta = 16:1$ ). This catalyst system is also amendable to the synthesis of a protected human milk  $\alpha$ -trisaccharide (**31**).<sup>[19]</sup>

The critical question remains whether the phenanthroline system could be applicable for the construction of larger oligosaccharides. To illustrate this potential, we examined the synthesis of the octasaccharide **40** (Scheme 2), a backbone of



**Scheme 2.** Synthesis of the octasaccharide **40**. a) 5–15 mol% of **4**, IBO (2 equiv), MTBE (2 M), 50 °C, 24 h, **34**: 89%,  $\alpha/\beta > 20:1$ ; **37**: 86%,  $\alpha/\beta > 20:1$ ; **40**: 77%,  $\alpha/\beta > 20:1$ ; b) NaOMe, MeOH, CH<sub>2</sub>Cl<sub>2</sub>, 25 °C, **35**: 99%, **38**: 70%; c) PTSA, Ac<sub>2</sub>O, 70 °C, 2 h (glycosyl acetates: **36S**: 61%, **39S**: 51%, see the Supporting Information); then HBr/AcOH, CH<sub>2</sub>Cl<sub>2</sub>, 0 °C, 15 min, and **36** and **39** were used in the next step without further purification. PTSA = *p*-toluene sulfonic acid.

the natural  $\alpha$ -glucan polysaccharides,<sup>[20]</sup> potential vaccine adjuvants. These  $\alpha$ -glucans are heterogeneous in size and composition. As such, well-defined oligosaccharides are required to study bioactive fragments. In our approach, a catalyst loading of 5 mol% proved efficient to promote the coupling of the commercially available **33** with the glycosyl bromide **32** to provide 8.4 grams of the product **34** in 89% yield with  $\alpha/\beta > 20:1$ . The disaccharide **34** was then converted into the glycosyl bromide **36**,<sup>[21]</sup> which was used in the coupling to **35** to afford the tetrasaccharide **37** (86%,  $\alpha/\beta > 20:1$ ). Another coupling iteration afforded **40** (77%,  $\alpha/\beta > 20:1$ ).

Having obtained the 1,2-*cis* product in high yield and  $\alpha$ -selectivity, we sought to investigate the mechanism of this catalytic glycosylation. We first attempted to detect a transient  $\beta$ -covalent phenanthroline ion using mass spectrometry. In the event, **1** was treated with a stoichiometric amount of **4** in MTBE (0.5 M) for 24 hours at 50 °C. Formation of the phenanthroline ion **41** (Figure 1A) was confirmed using electrospray ionization (ESI) with an *m/z* ratio of 711.2710.<sup>[22]</sup>

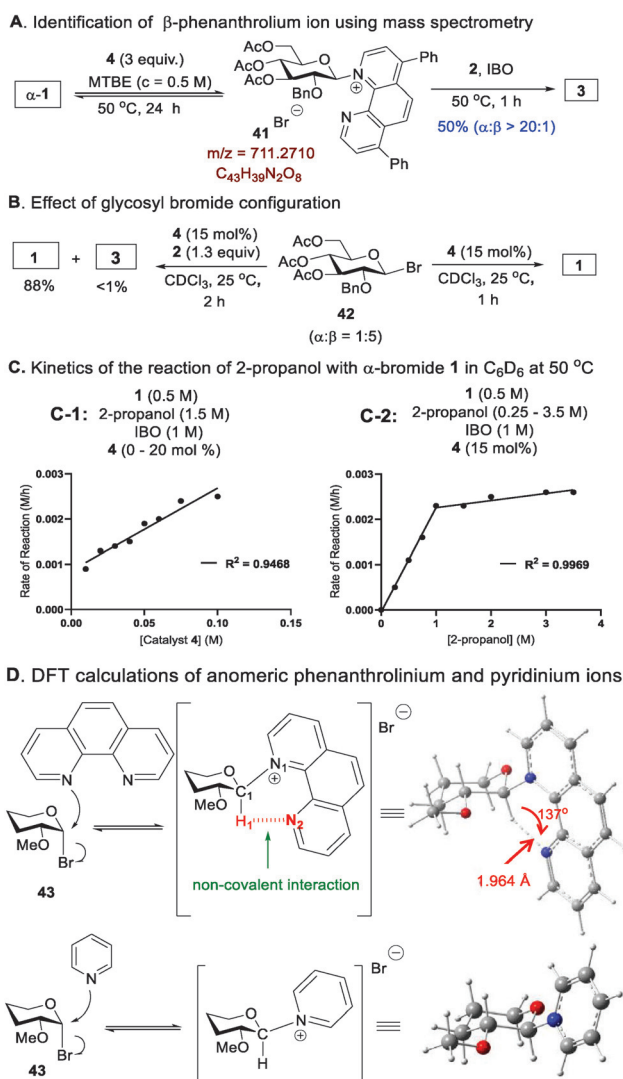


Figure 1. Mechanistic studies.

We next evaluated if the stereochemistry of the  $\alpha$ -1,2-*cis* product would be dictated by the anomeric configuration of the glycosyl bromide (Figure 1B).<sup>[23]</sup> We observed that the  $\beta$ -bromide **42**<sup>[24]</sup> only slowly isomerized to **1** without catalyst **4** (see Figure S10). However, **42** rapidly converted into **1** in the presence of 15 mol% of **4** within 1 hour at 25 °C (Figure 1B).<sup>[25]</sup> We also performed the reaction of **42** with the nucleophile **2** in the presence of **4**, and we observed that isomerization of  $\beta$ -**42** to  $\alpha$ -**1** is faster than formation of the product **3**.<sup>[26,27]</sup> Collectively, these results suggest that **42** is not the reacting partner in the phenanthroline system.

Next, kinetic studies were conducted at 50 °C, using  $C_6D_6$  as the NMR solvent and toluene as a quantitative internal standard, with **1** and 2-propanol as coupling partners in the presence of IBO and **4**. The rates of reaction were plotted as functions of the concentrations of **4** (Figure 1C-1) and 2-propanol (Figure 1C-2). Overall, the kinetic data suggest that the reaction proceeds by double  $S_N2$ -like mechanism (Figure 1C; see Figures S11–S15), as the rate of the reaction is both catalyst- and nucleophile-dependent. The biphasic kinetics in Figure 1C-2 suggest a shift in the rate-determining

step (RDS) at different concentrations of 2-propanol. At high concentration of 2-propanol, the RDS is formation of the phenanthrolium ion (first step in Scheme 1C), and is further supported by the linear dependence of rate on catalyst concentration (Figure 1C-1). At low concentration of 2-propanol, nucleophilic attack (second step in Scheme 1C) is the RDS.

Finally, to understand the role of the phenanthroline catalyst in controlling  $\alpha$ -1,2-*cis* glycosylation, the transition structures and intermediates for nucleophilic addition of either phenanthroline or pyridine to the  $\alpha$ -bromide **43** were optimized utilizing density-functional theory (DFT) calculations at the B3LYP/6–31 + G(d,p) level with the SMD implicit solvent model (Figure 1D; see Figure S16). Noncovalent interaction (NCI) analysis<sup>[28]</sup> (see Figure S18) indicates that the  $\beta$ -phenanthrolium ion is stabilized by interactions between the C1 axial hydrogen of the glycosyl moiety and the nitrogen center of phenanthroline (the  $H_1-N_2$  distance is 1.964 Å and the  $C_1-H_1-N_2$  angle is 137°).<sup>[29]</sup> NCI analysis, however, does not show corresponding interactions for the  $\beta$ -pyridinium ion. DFT calculations find that  $\beta$ -phenanthrolium ion is more stable than the  $\alpha$ -complex ( $\Delta G_{\beta \rightarrow \alpha} = +6.7$  kcal mol<sup>-1</sup>; see Figure S19), thereby shielding the  $\beta$ -face and favoring  $S_N2$  attack on the  $\alpha$ -face to yield  $\alpha$ -1,2-*cis* glycoside.

In conclusion, the phenanthroline-catalyzed glycosylation strategy provides a general platform for  $\alpha$ -selective formation of 1,2-*cis* glycosides under mild and operationally simple reaction conditions. This system is not confined to the predetermined nature of the coupling partners and mimics the glycosyltransferase-catalyzed mechanism. Our computational and experimental studies indicate a double  $S_N2$  pathway involving phenanthroline-catalyzed glycosylation with  $\alpha$ -glycosyl bromide. Efforts to utilize this method to enable other glycosidic bonds are underway.

## Acknowledgements

We are grateful for financial support from the National Institutes of Health (U01 GM120293). We thank Profs. David Crich (Wayne State) and Daniel Quinn (Iowa) for suggestions with kinetic studies as well as the Lumigen Center for instrumental assistance.

## Conflict of interest

The authors declare no conflict of interest.

**Keywords:** glycosylation · oligosaccharides · organocatalysis · reaction mechanisms · stereoselectivity

**How to cite:** *Angew. Chem. Int. Ed.* **2019**, *58*, 6957–6961  
*Angew. Chem.* **2019**, *131*, 7031–7035

[1] a) K. Ohtsubo, J. D. Marth, *Cell* **2006**, *126*, 855–867; b) Y. van Kooyk, G. Rabinovich, *Nat. Immunol.* **2008**, *9*, 593–601.

- [2] a) M. J. McKay, H. M. Nguyen, *ACS Catal.* **2012**, *2*, 1563–1595; b) M. M. Nielsen, C. M. Pedersen, *Chem. Rev.* **2018**, *118*, 8285–8358.
- [3] W.-L. Leng, H. Yao, J.-X. He, X.-W. Liu, *Acc. Chem. Res.* **2018**, *51*, 628–639.
- [4] a) J.-H. Kim, H. Yang, G.-J. Boons, *Angew. Chem. Int. Ed.* **2005**, *44*, 947–949; b) J.-H. Kim, H. Yang, J. Park, G.-J. Boons, *J. Am. Chem. Soc.* **2005**, *127*, 12090–12097; c) J. P. Yasomanee, A. V. Demchenko, *J. Am. Chem. Soc.* **2012**, *134*, 20097–20102; d) J. P. Yasomanee, A. V. Demchenko, *Angew. Chem. Int. Ed.* **2014**, *53*, 10453–10456.
- [5] a) Y. Geng, A. Kumar, H. M. Faidallah, H. A. Albar, I. A. Mhkalid, R. R. Schmidt, *Angew. Chem. Int. Ed.* **2013**, *52*, 10089–10092; b) S. Buda, M. Mawoj, P. Golebiowska, K. Dydach, A. Michalak, J. Mlynarski, *J. Org. Chem.* **2015**, *80*, 770–780; c) P. Peng, R. R. Schmidt, *J. Am. Chem. Soc.* **2015**, *137*, 12653–12659; d) T. Kimura, T. Eto, D. Takahashi, K. Toshima, *Org. Lett.* **2016**, *18*, 3190–3193; e) L. Sun, X. Wu, D.-C. Xiong, X.-S. Ye, *Angew. Chem. Int. Ed.* **2016**, *55*, 8041–8044; f) Y. Park, K. C. Harper, N. Kuhl, E. E. Kwan, R. Y. Liu, E. N. Jacobsen, *Science* **2017**, *355*, 162–166.
- [6] L. L. Lairson, B. Henrissat, G. J. Davies, S. G. Withers, *Annu. Rev. Biochem.* **2008**, *77*, 521–555.
- [7] a) R. U. Lemieux, A. R. Morgan, *J. Am. Chem. Soc.* **1963**, *85*, 1889–1890; b) R. U. Lemieux, A. R. Morgan, *Can. J. Chem.* **1965**, *43*, 2205–2213.
- [8] B. A. Garcia, D. Y. Gin, *J. Am. Chem. Soc.* **2000**, *122*, 4269–4279.
- [9] G. Lanz, R. Madsen, *Eur. J. Org. Chem.* **2016**, 3119–3125.
- [10] A. C. Spivey, S. Arseniyadis, *Angew. Chem. Int. Ed.* **2004**, *43*, 5436–5441.
- [11] S. S. Nigudkar, K. J. Stine, A. V. Demchenko, *J. Am. Chem. Soc.* **2014**, *136*, 921–923.
- [12] S. Chatterjee, S. Moon, F. Hentschel, K. Gilmore, P. H. Seeberger, *J. Am. Chem. Soc.* **2018**, *140*, 11942–11953.
- [13] S. R. Lu, Y. H. Lai, J. H. Chen, C. Y. Liu, K. K. T. Mong, *Angew. Chem. Int. Ed.* **2011**, *50*, 7315–7320.
- [14] D. Vasudevan, H. Takeuchi, S. S. Johar, E. Majerus, R. S. Haltiwanger, *Curr. Biol.* **2015**, *25*, 286–295.
- [15] P. C. Gao, S. Y. Zhu, H. Cao, J. S. Yang, *J. Am. Chem. Soc.* **2016**, *138*, 1684–1688.
- [16] M. R. Pratt, C. R. Bertozzi, *Chem. Soc. Rev.* **2005**, *34*, 58–68.
- [17] S. D. Kuduk, J. B. Schwarz, X.-T. Chen, P. W. Glunz, D. Sames, G. Ragupathi, P. O. Livingston, S. J. Danishefsky, *J. Am. Chem. Soc.* **1998**, *120*, 12474–12485.
- [18] a) C. Bucher, R. Gilmour, *Angew. Chem. Int. Ed.* **2010**, *49*, 8724–8728; b) E. Durantie, C. Bucher, R. Gilmour, *Chem. Eur. J.* **2012**, *18*, 8208–8215.
- [19] X. Chen, *Adv. Carbohydr. Chem. Biochem.* **2015**, *72*, 113–190.
- [20] a) A. L. van Bueren, M. Higgins, D. Wang, R. D. Burke, A. B. Boraston, *Nat. Struct. Mol. Biol.* **2007**, *14*, 76–84; b) V. C. B. Bittencourt, R. T. Figueiredo, R. B. da Silva, D. S. Mourao-Sa, P. L. Fernandez, G. L. Sasaki, B. Mulloy, M. T. Bozza, E. B. Barreto-Bergter, *J. Biol. Chem.* **2006**, *281*, 22614–22623.
- [21] Y. Cao, Y. Okada, H. Yamada, *Carbohydr. Res.* **2006**, *341*, 2219–2223.
- [22] Fragmentation of **41** using collision induced dissociation led to formation of phenanthroline with an *m/z* ratio of 333.1396 (see Figure S8).
- [23] Y. Singh, T. H. Wang, S. A. Geringer, K. J. Stine, A. V. Demchenko, *J. Org. Chem.* **2018**, *83*, 374–338.
- [24] R. U. Lemieux, K. B. Hendriks, R. V. Stick, K. James, *J. Am. Chem. Soc.* **1975**, *97*, 4056–4062.
- [25]  $\beta$ -**42** rapidly converted into  $\alpha$ -**1** in the presence of catalyst **4** within 15 min at 50 °C.
- [26] Coupling of **2** with **42** under standard reaction conditions provided **3** in comparable yield and  $\alpha$ -selectivity to that obtained with **1**.
- [27] The  $\alpha/\beta$  ratio of **3** is kinetically derived and is not reflective of a thermodynamic distribution arising from post-coupling isomerization (see Figure S9).
- [28] E. R. Johnson, S. Keinan, P. Mori-Sanchez, J. Contreras-Garcia, A. J. Cohen, W. Yang, *J. Am. Chem. Soc.* **2010**, *132*, 6498–6506.
- [29] The optimized geometry of the transition state shows that because of the backside displacement nature of the  $S_N2$  transition state, the distance is too large for any stabilizing interaction between the hydrogen atom of the alcohol and the nitrogen center of phenanthroline (see Figure S17).

Manuscript received: January 30, 2019

Revised manuscript received: March 7, 2019

Accepted manuscript online: March 28, 2019

Version of record online: April 9, 2019